M.D. Barath Kumar
M.Tech CAD/CAM
School of Mechanical Engineering
Vellore Institute of Technology
Vellore
India

K.M. Aravindan
M.Tech CAD/CAM
School of Mechanical Engineering
Vellore Institute of Technology
Vellore
India

A. Vinoth Jebaraj
Associate Professor
School of Mechanical Engineering
Vellore Institute of Technology
Vellore
India

T. Sampath Kumar
Associate Professor
School of Mechanical Engineering
Vellore Institute of Technology
Vellore
India

Effect of Post-Fabrication Treatments on Surface Residual Stresses of Additive Manufactured Stainless Steel 316L

In this work, an investigation was made to analyze the surface residual stresses on additive manufactured stainless steel AISI 316L in as-built and post-treated conditions. Direct metal laser sintering was used to fabricate the metal blocks. X-ray residual stress analysis on the as-fabricated surface revealed the presence of an inhomogeneous and irregular distribution of residual stresses in the as-built condition ranging from – 30 MPa to 111 MPa. It was mainly due to the localized laser heat source that caused variations in stresses at a lattice level. Heat treatment was performed for providing relief to the residual stress from the as-built condition showed significant relief of residual stress, which was lesser than 50% compared to as-built condition. Beneficial compressive residual stress induced by shot peening and lapping resulted in high magnitude compressive stresses on the surface. Also, homogeneous distribution of residual stress was found on the peened and lapped surface layer with an average of – 531 MPa and – 554 MPa, respectively.

Keywords: *Metal additive manufacturing, laser-based powder bed fusion, residual stress, stainless steel 316L, heat treatment, shot peening, lapping.*

1. INTRODUCTION

Additive Manufacturing (AM) is one of the modern-day manufacturing methods used in the manufacture of complex-shaped parts, particularly for those seen in aero engine applications, aircraft structural components, and bio-implants, etc. [1-5]. Among the available AM techniques, metal AM technology is more popular and cost-effective mainly due to scrap minimization and minimum manufacturing time involved in the part fabrication. It offers flexibility which leads to the manufacture of highly complex-shaped structures, which is not possible with the use of conventional manufacturing methods. In a laser-based powder bed fusion process, metal particles are getting fused through a high intensified narrow laser beam [6-9]. A steeper temperature gradient leads to the accumulation of residual stresses during the fabrication, which is a significant pitfall that needs rectification. Many times designers and production engineers stumble to arrive at a successfully fabricated part mainly due to build failure, which is just the detachment of a part from the build plate and supporting structures. The crucial factors that lead to build failure of AM parts are the incorrect design of the support structure, improper scanning pattern, and wrong build orientation. All these failures are directly related to the storage of stresses inside the part. Fatigue failures were reported in the past, mainly in the locations of tensile residual stresses, which acted as crack initiation sites in the regions of manufacturing defects [10]. Many researchers have attempted to analyze the residual stresses and their effect during the real-time application of additive manufactured components. Igor et al. reported the accumulation of stresses in AISI 316L and titanium alloy (Ti6Al4V) parts produced by a selective laser melting process [11]. The presence of higher thermal gradients between the layers causing nucleation of residual stresses was reported. Material inside the existing built portion dissipates heat more slowly than the outer surface, causing the resistance between the layers as well as within the layer, thereby leading to the storage of residual stresses.

In the metal AM process, laser scanning direction has a significant influence in the nucleation of residual stresses providing stresses of a higher magnitude in the scanning direction compared to the perpendicular direction [12]. Several researchers have reported the formation of in-built residual stresses in various metal AM processes, with variations in the magnitude of residual stresses concerning material and process parameters involved [13, 14]. Complete understanding of residual stress pattern is an essential need for metal AM processes, considering their significant role played in the life of a component and its performance [15] The existence of stress inside the component is not always bad. Sometimes it is desirable when the component has compressive residual stresses present to help a substantial improvement to life. In general, heat treatment is carried out to provide relief to in-built residual stresses on metal AM parts [16]. Also, the process parameters for heat treatment are not equivalent to heat treatment parameters for conventional wrought alloys. Many researchers have reported post-fabrication heat treatment providing relief to the residual stresses effectively [17,

Received: August 2020, Accepted: October 2020
Correspondence to: Dr. A. Vinoth Jebaraj
School of Mechanical Engineering,
Vellore Institute of Technology, Vellore, India.
E-mail: vinothjebaraj.a@vit.ac.in
doi: 10.5937/fme2101087B

18]. A few attempts made in the past showed that shot peening on metal AM parts exhibited the accumulation of high magnitude compressive stresses on the surface layer of the material [19-21]. Surface finishing using conventional machining processes has also been suggested to enhance the surface quality, and roughness parameters of metal AM parts [22, 23]. Minimal work has been carried out on the subject of the comparison of the surface residual stresses in the as-fabricated as well as post-treated conditions. It will be useful to compare the effect of post-fabrication treatments on the surface residual stresses in the metal AM specimens manufactured uniquely with the same process parameters. The focus of this study is on the influence of stress relief to heat treatment, shot peening, and lapping on the modification of surface residual stress pattern in AISI 316L fabricated through the use of a laser-based AM process.

2. EXPERIMENTAL DETAILS

The alloying elements of stainless steel 316L metal powder particles based on the EOS specification are shown in Table 1. The dimensions of the roughly spherical powder particles used in the sample fabrication were ranging from 4µm to 40µm.
The powder particles used in the present study were produced using an advanced atomization process in which the wire form raw material was inserted into the atomization chamber for melting as well as atomization into a spherical shape. Finally, the powder particles were collected at the bottom of the unit, and sieving was performed for classification of the powder according to the size.

Table 1. Chemical composition of stainless steel AISI 316L [19]

Elements	Cr	Ni	Cu	Mn	Si	Mo
Weight%	17.73	13.53	0.01	1.58	0.45	2.65
Elements	C	S	P	N	Fe	-
Weight%	0.007	0.006	0.010	0.07	Bal	-

2.1 Metal AM sample fabrication

The schematic view of the Direct Metal Laser Sintering (DMLS) machine used for sample fabrication is shown in Figure 1. During the fabrication, the ytterbium fiber laser was used for the fusion of particles. Laser scans were seen as the 1st layer in the x-direction, 2nd layer in the y-direction, and 3rd layer in the xy-direction and the same sequence was followed in all the subsequent layers. The laser scanning strategy during the layer by layer fabrication and the fabricated samples are shown in Figure 2 (a) and (b). The parameters used in the DMLS process are shown in Table 2.

Table 2. DMLS Process parameters for sample fabrication

Max building volume	250mm X 250mm X 325mm
Laser type	Ytterbium fibre laser
Power	195 W
Laser diameter	80 µm
Precision optics	F-theta-lens, high-speed scanner
Scanning speed	1083 mm/s
Process gas	Argon
Layer thickness	~20 µm
Powder bed temperature	80°C

Argon was used as shielding gas in a laser scanning environment. Metal blocks of AISI 316L with dimensions of 20 mm × 20 mm × 5mm were made using the EOS DMLS (EOSINT M280) machine in CTTC, Bhubaneswar, India. CAD model of the sample was converted to STL format followed by slicing using a magic rapid prototyping build processor. The slicing of the model was done in various directions such as X, Y, and XY directions, and these were saved in the STL file format and specified as input to the metal AM DMLS machine.

2.2 Post-processing treatments

Microstructural analysis was carried out in the as-built sample in which a small specimen of size 5x5 mm was extracted from the sample and polished using emery sheets in the order of decreasing surface roughness followed by disc polishing. After polishing, the sample was etched using an aquaregia solution.

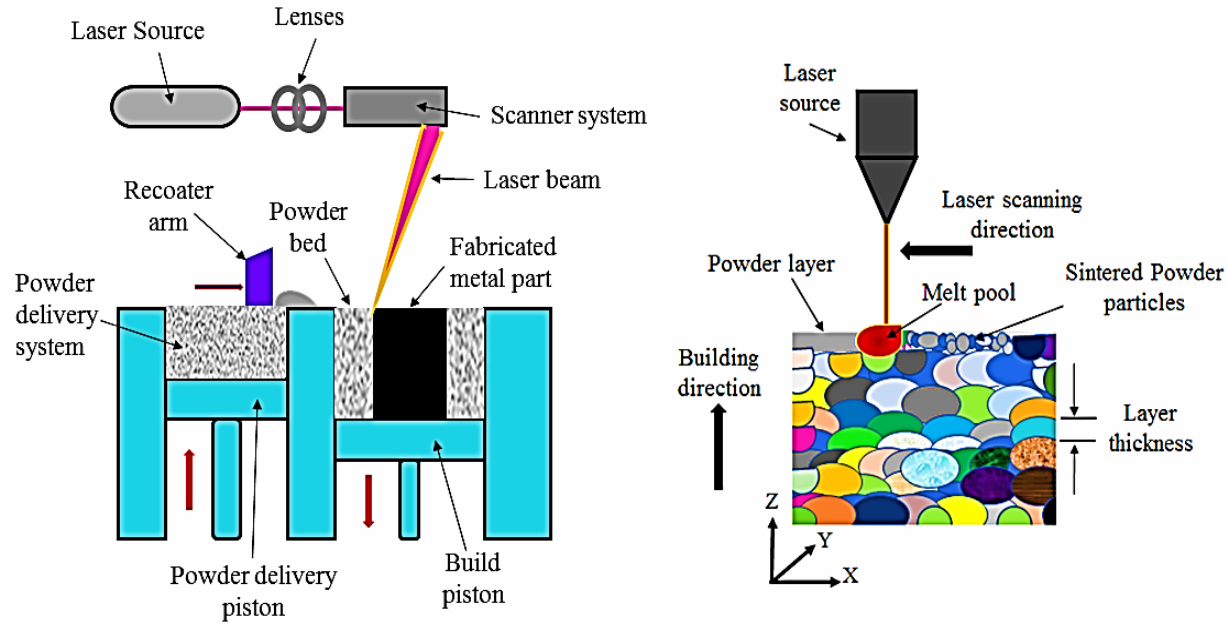

Figure 1. Schematic view of DMLS process

Heat treatment was carried out in a muffle furnace at a temperature of 210ºC in an argon inert environment for 6 hours. Further, as a part of the investigation, conventional mechanical peening was carried out on the heat-treated sample surface with the use of hard steel shots. The shots of S-330 grade were used for peening, and the impeller speed was set to 2800 rpm. Peening coverage of 200% was targeted during the shot peening process for obtaining spherical indentations on the entire surface area. Optimization of peening parameters was carried out by multiple trials of shot peening on conventional stainless steel samples with an objective of 200% coverage on the surface. As one of the goals of the present study, the sample surfaces were machined using conventional grinding, followed by the lapping process to reduce the roughness parameters and achieve a better surface finish.

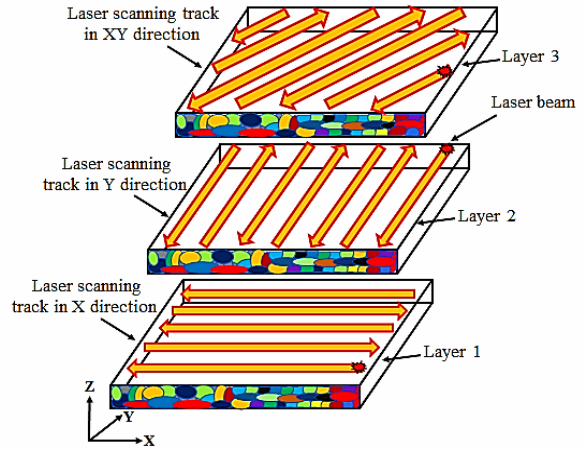

a) Scanning strategy

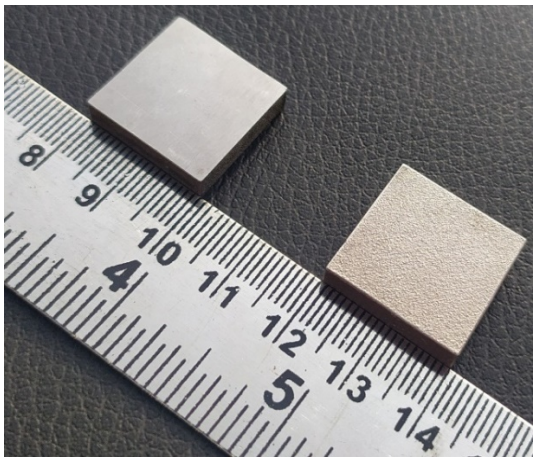

(b) Fabricated AISI 316L samples

Figure 2. Scanning directions and fabricated AISI 316L samples

2.3 Residual stress measurement

Residual stress measurement was carried out using non-destructive x-ray diffraction Cosα method. The use of a single-exposure x-ray provides residual stress values without tilting the sample, which is the major benefit of cosα method. In this method, two dimensional Debye ring was captured to calculate the residual strain on the sample surface, followed by stresses. If a material has no strain inside the crystal lattice structure, it will give a Debye ring, which is exactly the circular ring without any distortion. It indicates no residual stress. If the residual stress is present inside the material, there will be a residual strain in the lattice. Therefore the diffraction angle varies, which will lead to the distortion of the Debye ring. In the cosα method, strain ε_α at the Debye ring is used to measure the residual stress. The geometric representation of the Debye ring capturing process is shown in Figure 3. This method is more reliable because it captures many measuring points in the ring. The equation for measuring the residual stress is given as below:

$$\sigma_x = -\frac{E}{1+\nu}\frac{1}{\sin 2\eta}\frac{1}{\sin 2\psi_0}\left(\frac{\partial a_1}{\partial \cos\alpha}\right) \quad (1)$$

$$a_1 = \frac{1}{2}\left[\left(\varepsilon_\alpha - \varepsilon_{\pi+\alpha}\right)+\left(\varepsilon_{-\alpha} - \varepsilon_{\pi-\alpha}\right)\right] \quad (2)$$

where,
ε_α = Strain at Debye ring
E - Elastic modulus
ν - Poisson's ratio
α - Angle at the Debye ring
η - Diffraction angle between reflection line and input X-ray
ψ_0 - Orientation angle between normal line of sample and input X-ray

In the present study, residual stresses were measured in the as-built, heat-treated, shot-peened, and lapped samples. The measurement was taken at various locations on the top and bottom surfaces of the samples. Residual stress measurement device μ-X360 was used for mapping of the Debye Scherrer ring. This device is small as well as light for handling, and the measurement can be done in a short time compared to other methods. A gamma Fe (311) plane with K-beta wavelength was used for the measurement. The detailed mathematical procedure for calculating the residual stresses using cosα method is available in the following literature [24 – 28].

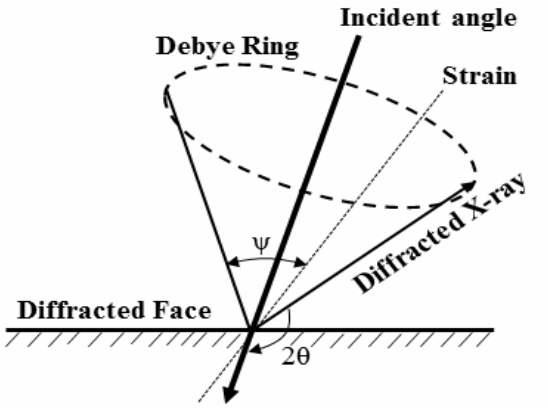

Figure 3. Geometric representation of Debye ring capture

3. RESULTS AND DISCUSSIONS

3.1 Microstructural Analysis

In the metal AM process, the AISI 316L powder particles were sintered together using a high intensified laser beam. The powder particles used in this process,

as-built surface morphology, and the microstructures of fabricated metal blocks are shown in Figure 4 (a) to (d). The microstructure reveals the austenite phases with overlapping grain boundaries. Over-lapping of grains was observed mainly as a result of the remelting of a previously solidified layer. The overlapping grains were seen to show elliptical grain boundaries arising from the focus of the intense laser beam delivered the Gaussian distribution of the laser energy. No secondary phases in the microstructure were seen, and the outer surface layers of the fabricated sample showed a large unit of peaks in the as-fabricated condition. The final layer of powder bed fusion left the sedimentation of unmelted and partially fused particles on the surface layer. This is a significant pitfall in the laser-based AM processes that need to be addressed. No major crack was seen, nor any macro-level dimensional change in the as-fabricated sample by the effect of rapid cooling action experienced in layer-wise fabrication. However, pores of a microscopic scale within the grains were seen. This was due to the entrapment of gases during laser scanning.

3.2 Comparison of residual stresses before and after heat treatment

Stress measurement was performed on the top surface layer of the as-fabricated and heat-treated samples. Non-uniform cooling of the solidifying track leads to the formation of residual stresses in AM parts. The scale of residual stress distributed on the surface layers with significant variations at different locations in the as-built sample was seen. Storage of uneven magnitude of residual stresses was the result of the localized action of a high intensified laser beam, which showed variations in stresses at the lattice level. The presence of a higher thermal gradient between the layers was the reason for the inhomogeneous distribution of residual stresses in the as-fabricated condition. The average value of residual stresses in the as-built surface was almost 30% of the material's yield strength. There were variations in the nature of stress from tensile to compressive in one of the measured locations of the outer surface. This was the result of the localized shrinkage provided by the moving heat source. Literature has reference to this investigation carried out by Michael et al., which revealed compressive stresses on the bottom surface and tensile residual stresses on the top surface, in the AM made part [29].

The measurement revealed tensile stresses in most of the locations of the sample. The residual stress values on the as-built surface at various locations were obtained as slopes of lines plotted between the normal strain and cosα, which is shown in Figure 5 (a). The residual stress gradient observed on the surface shows the inapplicability of the fabricated part using DMLS for critical applications without any stress-relieving heat treatment. Lesser fatigue strength was reported for additive manufactured parts in the as-built condition than the annealed sample. However, this is not true for all the metals fabricated by the AM processes as the fatigue failure mechanism varies concerning the ductility of the materials.

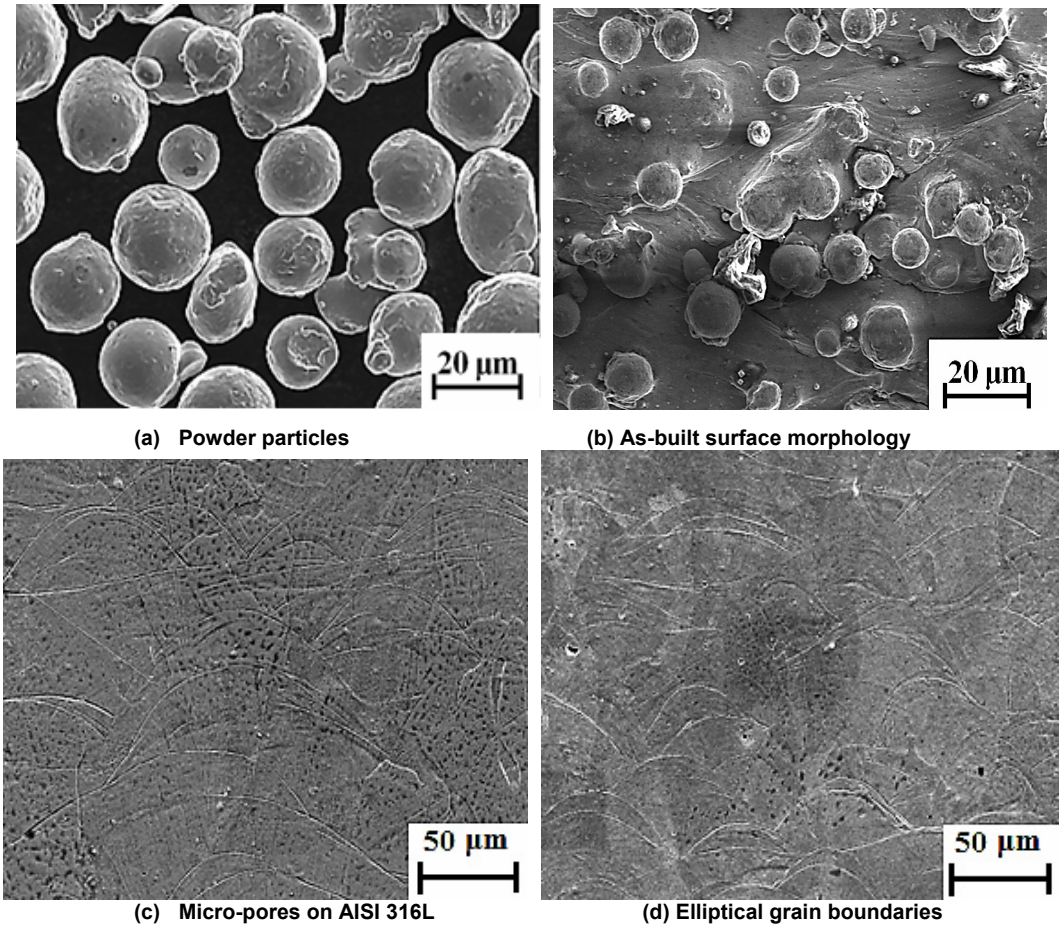

(a) Powder particles (b) As-built surface morphology

(c) Micro-pores on AISI 316L (d) Elliptical grain boundaries

Figure 4. Microstructure Analysis of AISI 316L

Sometimes, lesser fatigue strength was reported even after the post-annealing, which was mainly due to the domination of voids present [10, 30]. The residual stress values of heat-treated samples showed that there was significant relief in the residual stress in the material following the heat treatment. Heat treatment for a prolonged duration resulted in the tempering of a sample triggering relief of residual stresses. The residual stress values after heat treatment obtained were in the form of slopes of lines plotted between the normal strain and cosα, which is shown in Figure 5(b). There was a reduction in the slope after heat treatment compared to the as-built condition. The average reduction of residual stresses in the heat-treated sample showed a 65% reduction compared to that of the as-built sample.

3.1. Effect of shot peening and lapping

Shot peening resulted in compressive residual stresses at all locations of the surface. The magnitudes of compressive residual stresses at different locations were seen as very high showing homogeneous distribution all over the peened surface. The 200% peening coverage and uniform hitting of shots are also the major factors for the uniform distribution of residual stresses. The present study recommends shot peening as the essential requirement for components made using metal AM processes. The presence of compressive residual stress improves fatigue life [10]. Literature also shows the significant benefits of shot peening on DMLS fabricated metal part, which produces improvement in surface properties and corrosion resistance [31]. The residual stress values on the shot-peened surface at various locations are shown in Figure 6(a). A significant improvement in the slope values of the normal stress plots compared to the as-fabricated and heat-treated specimens was seen.

Lapping also resulted in the accumulation of compressive stresses on the surface. The average value of residual stresses induced by the lapping process was seen almost equal to the peening induced residual stresses. However, the cost of the lapping process was comparatively higher than that of the shot peening process. The residual stress plots display observations of a lapped surface similar to the peened surface, which is shown in Figure 6(b). Full-width half maximum (FWHM) values obtained from the peened sample proved the existence of severe plastic deformation and slip bands on the peened surface layer. The FWHM values of shot-peened samples showed an increase to twice compare to the as-built and heat-treated samples. A comparison of FWHM values of post-treated samples with an as-built sample is shown in Figure 7. In general, metal AM processes lead to the nucleation of fine grains due to rapid cooling action experienced in layer-wise fabrication. Shot peening causes improvement in grain refinement due to the high-velocity impact of the hard steel shots on the surface.

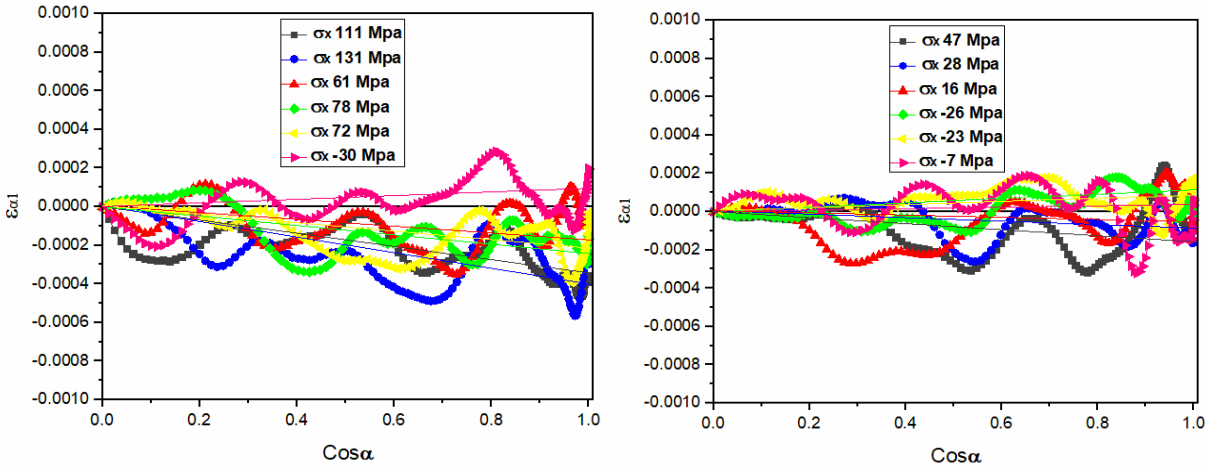

Figure 5. Residual stress values (a) as fabricated sample (b) heat treated sample

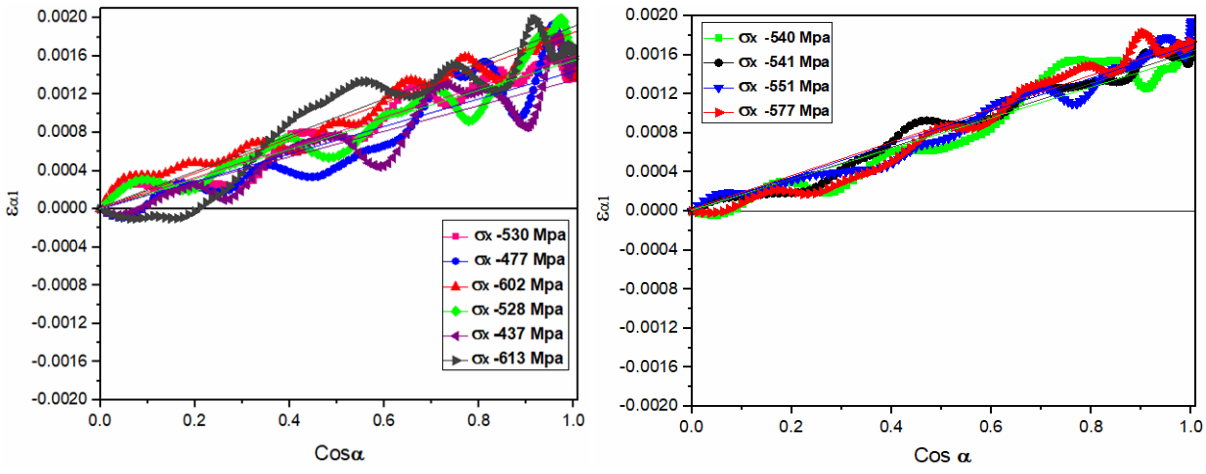

Figure 6. Residual stress values (a) shot peened surface (b) lapped surface

Bandar et al. have reported grain refinement following the shot peening process, which improved the surface quality of the parts fabricated through the metal AM process [20]. The Debye rings obtained from the X-ray residual stress analysis for all the samples are shown in Figure 8 (a) to (d). Debye rings obtained from shot-peened and lapped samples showed uniform intensity around the circumference compared to as-fabricated and heat-treated samples. It is mainly because of the uniform compression of the surface layers induced by peening and lapping processes. The broadening of peaks observed were the results of the microstrain and reduction in grain size.

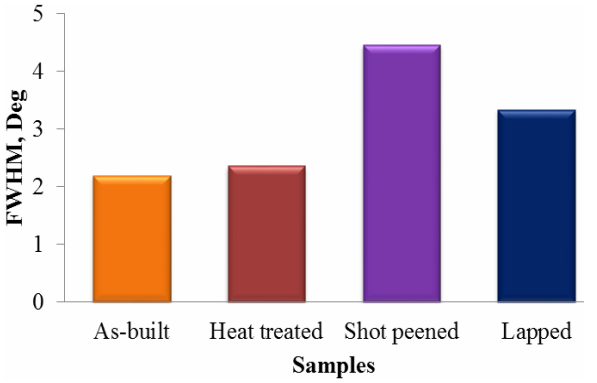

Figure 7. FWHM values of shot peened surface compared to other surfaces

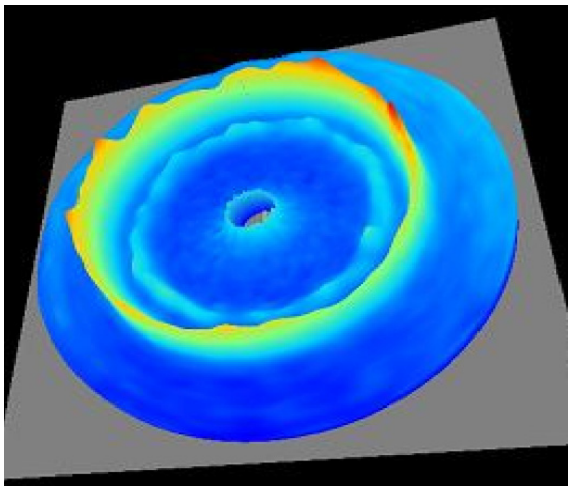

a) As-fabricated sample

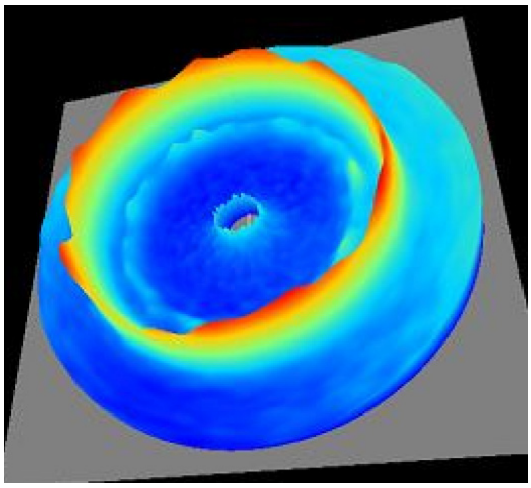

b) Heat treated sample

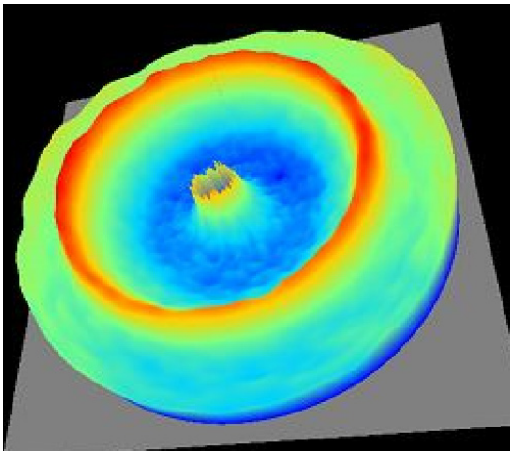

c) Shot peened surface

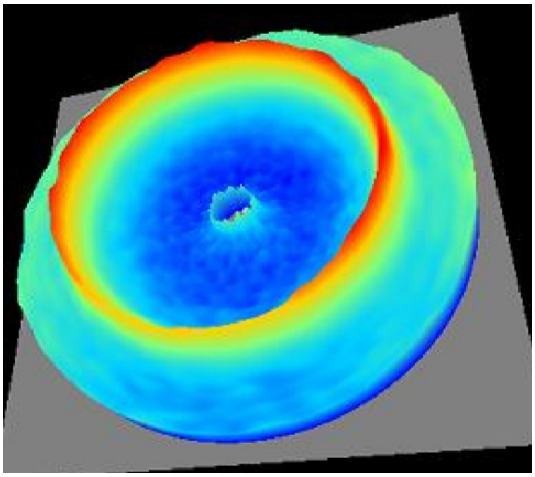

d) Lapped surface

Figure 8. Debye rings of various surfaces

4. CONCLUSION

The present study reveals the analysis of residual stresses on metal blocks of AISI 316L fabricated using the laser-aided additive manufacturing process. The following observations have been made on the samples in the as-built and post-treated conditions such as heat treatment, shot peening and lapping.

In the as-built sample surface, uneven magnitudes of residual stresses such as 111 MPa, 78 MPa, 131 MPa, 72 MPa, 61 MPa, and – 31 MPa have been observed at various locations. Most of the locations on the sample surface exhibited the tensile nature of residual stresses. Higher thermal gradients and a rapid cooling process led to the storage of heterogeneous distribution of stresses. A reduction in the magnitudes of surface residual stresses to 47 MPa, -26 MPa, 28 MPa, - 23 MPa, 16 MPa and – 7 MPa was seen following heat treatment. The provision of stress relief treatment played a major role in reducing the residual stresses present in the as-fabricated condition. The findings here show the usage of SS 316L AM parts without stress relieving heat treatment is not advisable as it may lead to a catastrophic failure of the parts.

Shot peening led to the storage of compressive residual stresses such as – 530 MPa, - 528 MPa, - 477 MPa, - 437 MPa, - 602 MPa, - 613 MPa on the surface layer. The magnitude of the average value of compressive

residual stress measured on the peened surface showed higher values of stresses, which were four times those seen on the as-built sample. The compressed surface layer of the shot-peened AM sample acts as a protective skin and will be helpful in delaying the crack initiation from the surface during service. Further, shot peening resulted in an increase in FWHM values to twice the amount from the as-built condition. The magnitudes of surface compressive residual stresses that the lapping process brought were almost equal to those of shot peening such as - 540 MPa, - 547 MPa, - 551 MPa, - 577 MPa. The findings of the present investigation will be useful in the mitigation of residuals stresses of SS 316L parts fabricated by AM processes.

As a future scope of study, the multistage shot peening will be performed and its effect on the improvement of surface residual stress pattern of AM metallic samples will be investigated. Also, the usefulness of laser shock peening on the enhancement of surface properties of AM metallic samples will be attempted.

ACKNOWLEDGMENT

Authors wish to thank VIT University for the constant encouragement and motivation in publishing this article. Authors also wish to thank the lab in-charge of advanced materials processing and testing lab, VIT Vellore for the facility provided to carry out this research work.

REFERENCES

[1] Murr, L.E. et al.: Metal fabrication by additive manufacturing using laser and electron beam melting technologies, J. Mat. Sci. Tech, vol. 28, No.1, pp. 1 – 14, 2012.

[2] Townsend, A., Senin, N., Blunt, L., Leach, R.K., Taylor, S.: Surface texture metrology for metal additive manufacturing: a review, Prec. Eng, Vol. 46, pp. 34 – 47, 2016.

[3] Kaufui V. Wong**,** Aldo Hernandez.: A Review of Additive Manufacturing, International Scholarly Research Network ISRN Mechanical Engineering, Article ID 208760, pp. 1- 10, 2012.

[4] Zivanovic, S.T., Popovic, M.D., Vorkapic, N.M., Pjevic, M.D., Slavkovic, N.R.: An Overview of Rapid Prototyping Technologies using Subtractive, Additive and Formative Processes, FME Trans., Vol. 48, No.1, pp. 246-253, 2020.

[5] M. Sljivic, A. Pavlovic, M. Stanojevic, C. Fragassa,: Combining Additive Manufacturing and Vacuum Casting for an Efficient Manufacturing of Safety Glasses, FME Trans., Vol. 44, No. 4, pp. 393-397, 2016.

[6] I. Gibson, D.W. Rosen, B. Stucker, *Additive manufacturing technologies*, 2nd Edition, Springer Publications, ISBN: 978-1-4419-1120-9.

[7] L. Bian, N. Shamsaei, J. Usher, *Laser-Based Additive Manufacturing of Metal Parts*, CRC Press Taylor & Francis Group, ISBN: 9781315151441.

[8] Dongdong Gu, *Laser Additive Manufacturing of High Performance Materials*, Springer Publisher, ISBN: 978-3-662-46089-4.

[9] Simchi, A., Petzoldt, F., Pohl, H.: On the development of direct metal laser sintering for rapid tooling, J. Mat. Proc. Tech., vol. 141, No.3, pp. 319 – 328, 2003.

[10] Aref Yadollahi, Nima Shamsaei.: Additive manufacturing of fatigue resistant materials: Challenges and opportunities, Int. J. Fat., vol. 98, pp. 14 – 31, 2017.

[11] Igor Yadroitsev, Ina Yadroitsava.: Evaluation of residual stress in stainless steel 316L and Ti6Al4V samples produced by selective laser melting, Virt Phy Proto, vol. 10, No. 2, pp. 67 – 76, 2015.

[12] Thomas Simson, Andreas Emmel, Anja Dwars, Juliane Böhm.: Residual stress measurements on AISI 316L samples manufactured by selective laser melting, Addi. Manu., vol. 17, pp. 183 – 189, 2017.

[13] Sochalski-Kolbus, L.M., Payzant, E.A., Cornwell, P.A., Watkins, T.R., Babu, S.S., Dehoff, R.R., Lorenz, M., Ovchinnikova, O., Duty, C.: Comparison of Residual Stresses in Inconel 718 Simple Parts Made by Electron Beam Melting and Direct Laser Metal Sintering, Meta. Mat. Trans. A, Vol. 46, No. 3, pp. 1419 – 1432, 2015.

[14] Albert E. Patterson, Sherri L. Messimer, Phillip A. Farrington.: Overhanging Features and the SLM/DMLS Residual Stresses Problem: Review and Future Research Need, Tech, Vol. 5, No. 15, pp. 1 – 21, 2017.

[15] Xiaoqing Wang, Kevin Chou.: Residual Stress in Metal Parts Produced by Powder-Bed Additive Manufacturing Processes**,** Annual International Solid Freeform Fabrication Symposium - An Additive Manufacturing Conference, pp. 1463 – 1474, 2015.

[16] Tatsuaki Furumoto, Takashi Ueda, Mohd Sanusi Abdul Aziz, Akira Hosokawa, Ryutaro Tanaka.: Study on Reduction of Residual Stress Induced during Rapid Tooling Process: Influence of Heating Conditions on Residual Stress, Key Eng. Mat., vol. 447-448, pp. 785 – 789, 2010.

[17] Anna Guzanova, Gabriela Izarikova, Janette Brezinova, Jozef zivcak, Dagmar Draganovska, Radovan Hudak.: Influence of Build Orientation, Heat Treatment, and Laser Power on the Hardness of Ti6Al4V Manufactured Using the DMLS Process, Met., vol. 7, No. 318, pp. 1 – 17, 2017.

[18] Shiomi, M., Osakada, K., Nakamura, K.: Yamashita T, Abe F, Residual Stress within Metallic Model Made by Selective Laser Melting Process, CIRP Annals, vol. 53, No. 1, pp. 195 – 198, 2004.

[19] Sugavaneswaran, M., Vinoth Jebaraj, A., Barath Kumar, M.D., Lokesh, K., John Rajan, A.: Enhancement of surface characteristics of direct metal laser sintered stainless steel 316L by shot peening, Surf. Inter. Vol. 12, pp. 31 – 40, 2018.

[20] Bandar Almangour, Jenn-Ming Yang.: Integration of Heat Treatment with Shot Peening of 17-4 Stainless Steel Fabricated by Direct Metal Laser Sintering, J. Miner. Met. & Mat. Soc., vol. 69, No. 11, pp. 2309 – 2313, 2017.

[21] Ahmed, H. Maamoun., Mohamed, A. Elbestawi., Stephen, C. Veldhuis.: Influence of Shot Peening

on AlSi10Mg Parts Fabricated by Additive Manufacturing, J. Manu. Mat. Proc., vol. 2, No. 40, pp. 1 – 16, 2018.
[22] Zhibo Yang, Mingjun Zhang, Zhen Zhang, Aiju Liu, RuiYun Yang, Shian Liu.: A study on diamond grinding wheels with regular grain distribution using additive manufacturing (AM) technology, Mat. Des., vol. 104, pp. 292 – 297, 2016.
[23] Konečná, R., Nicoletto, G., Fintová, S., Frkáň, M.: As-built surface layer characterization and fatigue behaviour of DMLS Ti6AL4V, Struc. Integ. Proc., vol. 7, pp. 92 – 100, 2017.
[24] Ami Kohri, Yasuhiro Takaku, Masashi Nakashiro.: Comparison of X-Ray Residual Stress Measurement Values by Cos α Method and Sin^2 Ψ Method, International conference on residual stresses ICRS – 10, Mat. Res. Proc., vol. 2, pp. 103 – 108, 2016.
[25] Sasaki, T.: New Generation X-Ray Stress Measurement Using Debye Ring Image Data by Two-Dimensional Detection, Mat. Sci. Forum., vol. 783 – 786, pp. 2103 – 2108, 2014.
[26] Ramirez-Rico, J., Lee, S.Y., Ling, J.J., INoyan, I.C.: Stress measurement using area detectors: a theoretical and experimental comparison of different methods in ferritic steel using a portable X-ray apparatus, J. Mat. Sci., vol. 51, No. 11, pp. 5343 – 5355, 2016.
[27] K. Tanaka.: The cos α method for X-ray residual stress measurement using two-dimensional detector, Mech. Eng. Rev., vol. 6, No. 1, pp. 1 – 15, 2019.
[28] J. Lin, N. Ma, Y. Lei, H. Murakawa.: Measurement of residual stress in arc welded lap joints by cos α X-ray diffraction method, J. Mat. Proc. Tech. vol. 243, pp. 387 – 394, 2017.
[29] Michael F. Zaeh, Gregor Branner.: Investigations on residual stresses and deformations in selective laser melting, Prod. Eng., vol. 4, pp. 35 – 45, 2010.
[30] Todd M. Mower, Michael J. Long.: Mechanical behaviour of additive manufactured, powder-bed laser-fused materials, Mat. Sci. Eng. A., vol. 651, pp. 198 – 213, 2016.
[31] Vinoth Jebaraj, A., Sugavaneswaran, M.: Influence of Shot Peening on Residual Stress Distribution and Corrosion Resistance of Additive Manufactured Stainless Steel AISI 316L, Trans. Ind. Inst. Met., vol. 72, No. 6, pp. 1651 – 1653, 2019.

УТИЦАЈ ПОСТУПКА НАКОН ИЗРАДЕ НА ПОВРШИНСКИ ЗАОСТАЛИ НАПОН КОД НЕРЂАЈУЋЕГ ЧЕЛИКА 316L ПРОИЗВЕДЕНОГ АДИТИВНИМ ПОСТУПКОМ

М.Д.Б. Кумар, К.М. Аравиндан, А.В. Ћебарај, Т.С. Кумар

Истражује се резидуални напон на површини нерђајућег челика AISI 316L произведеног адитивним поступком у условима извођеног поступка и након изведеног поступка. Директним ласерским синтеровањем метала израђени су метални блокови. Анализа резидуалног напона помоћу X-зрака на изведеној површини указала је на присуство нехомогене и неправилне дистрибуције заосталих напона у условима изведеног поступка – од 30 MPa до 111 MPa, што је углавном била последица локализованог ласерског извора топлоте који је узроковао варијације напона на нивоу мреже. Термички поступак изведен у циљу ослобађања заосалог напона у условима изведеног поступка имао је значајног ефекта и напон је био смањен за 50%. Користан притисни заостали напон изазван бомбирањем и пресликавањем имао је за последицу притисни напон велике јачине на површини. Нађена је хомогена дистрибуција заосталог напона на бомбираном и пресликаном површинском слоју, која је износила -531 MPa односно -554 MPa.